

# Enhancing Scanning Performance of Near-Field Planar Systems With Irregular Multi-probe Technology

E. Oblitas<sup>1,2,3</sup> and J. L. Salazar-Cerreno<sup>1,2,3</sup>

<sup>1</sup>Advanced Radar Research Center (ARRC)

<sup>2</sup>eMWave-Tech, Norman, OK, U.S.

<sup>3</sup>The University of Oklahoma, Norman, OK, U.S.

**Abstract**—This paper presents a novel design for a multi-probe antenna array for continuous measurement in a planar near-field system. This design reduces scanning time while maintaining accuracy compared to conventional methods used in near-field planar systems. The work introduces the design of the irregular probe array and discusses its trade-offs and functionality. It includes a comparison of the results from the two methods mentioned and analyzes the time durations associated with each approach. Additionally, the paper provides projections based on previous data to estimate scan durations for a large number of sampling points, considering the impact of the velocity of the linear positioners.

**Index Terms**—array antennas, faster scan process, multi-probe, near-field scan, planar near-field

## I. INTRODUCTION

Over the past few decades, near-field planar measurement systems have become essential for characterizing large antenna arrays with high gain, electronic scanning (e-scan) capabilities, and dynamic control of sidelobes and beams [1], [2]. These systems are particularly crucial in radar applications, where large arrays, often consisting of several thousand elements, require meticulous characterization and calibration. This process involves detailed pattern measurements, which are complex and time-consuming, often requiring several hours of testing to ensure accuracy and reliability. Currently, the planar near-field measurement system market is predominantly occupied by single-probe systems, favored for their simplicity. For instance, linear positioners move the probe antenna to specific positions, allowing for the creation of magnitude and phase maps. Although this technique is highly precise, it is time-consuming. To address this, continuous measurement systems have been developed over the years. Despite these advancements, the increasing demand for rapid and precise antenna measurements underscores the need for further innovation in near-field planar systems to reduce testing times without compromising data quality. Recent advancements have focused on leveraging compressed sensing and multi-probe systems to tackle these challenges. However, there are still numerous opportunities for further improvement [3].

New methods and techniques are continually being developed to reduce scanning durations and enhance measurement accuracy. While the concept of compressive sensing is rel-

atively established, its application in antenna measurements is quite novel [4]. This technique significantly reduces the number of sampling measurements required for near-field calculations. On the hardware front, advancements in linear and circular actuators have markedly improved their speed and accuracy over the years. Additionally, the emergence of robotic actuators, which offer versatility across various applications, including near-field scanning, represents a significant technological leap [5], [6]. Among the most promising solutions is the use of multi-probe antennas. Multi-probe near-field systems have proven highly effective in reducing scan durations. Reference [3] indicates that these systems can achieve a reduction in scan duration by a factor of 5 to 10, depending on factors such as the size, number of probe antennas, and test frequency. Other studies have explored error sources in planar near-field scans using multi-probe systems [7]. Additionally, research has examined alternative approaches to positioning systems, such as using wide grids to reduce the number of measurement points [8] or employing spiral paths to minimize the effects of strong acceleration and deceleration in probe arrays [9].

This paper presents the implementation of a continuous near-field raster scan utilizing a multi-probe irregular array design. This approach notably reduces scanning time while ensuring high measurement reliability. The subsequent sections will provide a detailed overview of the system components and their functionality. Additionally, the design considerations and trade-offs associated with the irregular probe-array antenna are discussed, along with the presentation of measurement results.

## II. SYSTEM DESCRIPTION AND REQUIREMENTS

This paper presents an automated system designed to measure electromagnetic properties in the near-field region of a planar section using multiple probe antennas. This approach significantly enhances measurement speed. To enable movement of the probe subsystem along the  $x$ - and  $y$ -axes, the system utilizes two linear positioners, specifically two VELMEX screw-driven actuators. The RF instrument used for measuring electromagnetic characteristics is a Copper Mountain vector network analyzer (VNA) with two RF ports. One port connects to the antenna under test (AUT) through an amplifier that compensates for system losses, while the other port connects

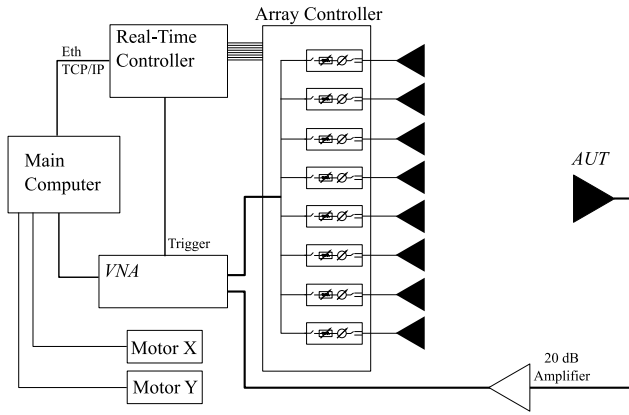


Fig. 1. Diagram of the multi-probe array scanning system.

to the array controller. The array controller manages element switching and controls the magnitude and phase in the probe antenna array. It features eight channels, each with two RF output ports for dual-polarization antennas. Each channel includes two serially connected 8-bit registers that store phase shifting, attenuation, polarization, and activation data. The array controller's phase shifters and attenuators are digitally controlled. The attenuator provides up to 32 dB of attenuation, and the phase shifter operates within a  $360^\circ$  range. Both components have 6-bit resolution, resulting in a minimum attenuation resolution of 0.5 dB and a phase shift resolution of  $5.625^\circ$ . The real-time controller (RTC) sends the necessary digital signals to the array controller to ensure proper operation with each state change.

The RTC is an embedded system responsible for configuring the array controller, managing timing and delays, and sending a digital signal to the VNA to initiate measurements upon detecting a rising edge signal from the RTC. In near-field planar scanning measurements, probe antennas must have low gain and a wide beam. As noted in [10], the open-ended waveguide antenna (OEWG) is commonly used for this purpose. For the S-band frequency range, the OEWG antenna with WR284 size operates between 2.60 and 3.95 GHz, with dimensions of 72.136 mm in width and 34.036 mm in height [11]. In this range, the minimum wavelength ( $\lambda$ ) is 75.9 mm, with half-wavelength being 37.95 mm. To construct an array of OEWG antennas, a separation of at least  $1\lambda$  is required. However, finding or fabricating probes with these specifications is challenging. Therefore, this paper uses dual-polarized patch antennas instead of OEWG antennas. The patch antennas fit within  $\lambda/2$  separation and perform well in both polarizations.

### A. System Functionality

As described earlier, the system components are interconnected as shown in Fig. 1. The main computer serves as the central processor, configuring all instruments and components, sending commands, and collecting data. It communicates with the RTC via TCP/IP. The main computer calculates positions,

calibration, and timing parameters, which it sends to the RTC. Using these timing parameters, the RTC manages probe switching and VNA triggering. The RTC initiates the process by sending a 5-volt trigger signal to the VNA at the precise moment. It then sends a bit chain to the array controller to activate the appropriate probe element, waits until the element is correctly positioned, and triggers the VNA. Once the VNA completes the measurement, the RTC signals the main computer, which then collects the data. The RTC immediately switches to the next element and repeats the process for the entire array. After completing measurements for all elements in the current column, the RTC proceeds to the next column in the scan grid.

### B. Multi-probe Array Design and Trade-offs

This system performs continuous planar near-field scan measurements using a probe array and a switching system. To minimize delays caused by switching, the probe array requires an innovative design. Key design parameters include the operating wavelength ( $\lambda$ ), the number of elements in the probe array ( $n_e$ ), and the speed of the positioners ( $v$ ).

$$\lambda/2 > \Delta d \cdot (n_e - 1) \quad (1)$$

$$v_{max} = \frac{\Delta d}{\Delta t_{min}} \quad (2)$$

$$\Delta t = \frac{\Delta d}{v} \quad (3)$$

To design the horizontal separation, we need to adhere to the constraint in (1). The maximum distance between elements must not exceed  $\lambda/2$ . If this distance is too large, the initial element may miss the next position while the last element is taking a measurement. The minimum time required for the RTC to switch from one element to another is denoted as  $t_{min}$ . The array controller used in this system has a minimum switching time of 25 ms, and the chosen horizontal separation ( $\Delta d$ ) is 2.5 mm. Using (2), we calculate that the maximum speed for the linear positioner, given this spacing, is 10 cm/s.

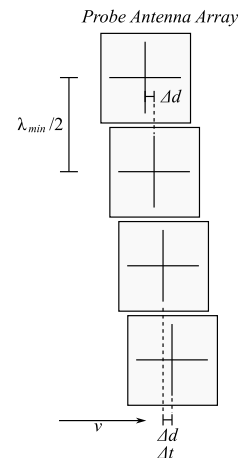


Fig. 2. Design of the probe antenna array, defining the spacing between the element of the array.

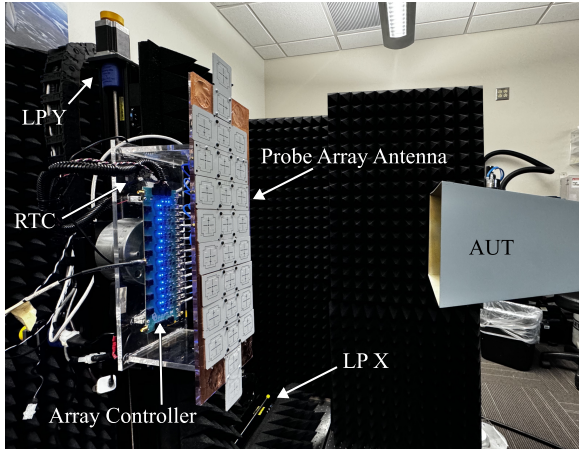


Fig. 3. Image of the system pointing most of the components of the system, LPX and LP Y are the linear positioners in x-axis and y-axis respectively.

It is not advisable to operate the linear positioner at maximum speed. According to (3), the RTC must wait for a certain time before triggering the next element. With a maximum velocity for the linear positioner set at 20 mm/s, this results in a waiting time ( $\Delta t$ ) of 125 ms.

Figure 2 displays the irregular antenna probe array, while Fig. 3 shows the developed system with the irregularities of the probe antenna array clearly visible. The probe array, composed of patch antennas, includes additional elements adjacent to the central ones. These non-connected and terminated elements, known as dummy elements, are crucial for near-field measurements with multi-probe systems. Dummy elements are necessary to ensure that the electromagnetic properties—such as magnitude, phase, and radiation pattern—are as uniform as possible across all elements. While achieving perfect uniformity is challenging, calibration can bring the elements' properties close to identical. The dummy elements help mitigate refraction and edge effects of the patch antennas, contributing to a more uniform and stable radiation pattern for the central elements.

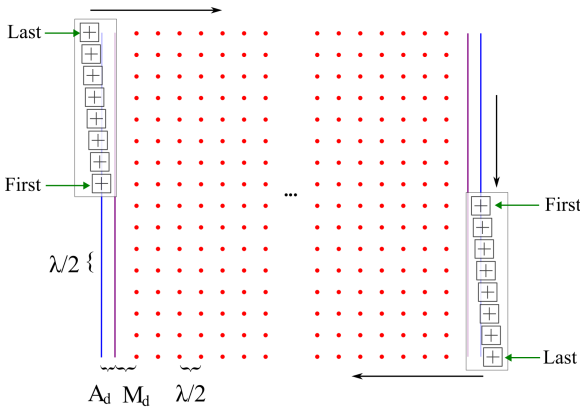


Fig. 4. Diagram of scanning points with the probe antenna array.

### C. Probe Array Calibration

Ideally, all antennas in the probe array should have identical electromagnetic properties. However, in practice, components are not perfect and can exhibit variations that significantly impact measurements. To minimize these discrepancies, the array controller can digitally adjust the magnitude and phase of each element. The calibration process is straightforward. An antenna is placed in front of each element, and the array controller enables the corresponding element. To prevent reflections or coupling from nearby antennas, the attenuation of all other elements is set to -30 dB, reducing any reflections captured by adjacent antennas to an insignificant level. After an initial measurement of the entire array, the main computer identifies the measurement with the lowest magnitude, as there are only attenuators and no amplifiers, and selects this as the phase reference. The positioners then reposition the probe array to reverse the process. During this step, the software continuously measures and adjusts the magnitude and phase of each element until the measurements closely match the reference values. The degree of acceptance depends on the resolution of the attenuator and phase shifter. In this system, the attenuator and phase shifter have resolutions of 0.5 dB and  $5.625^\circ$ , respectively. This results in a minimal margin of error, which is assumed to have a negligible impact on the measurements. This calibration process is repeated for each element in the probe array, and the resulting data is stored in a file for use in the near-field scanning process.

### D. Scanning Process

The process begins with the main computer configuring all system devices and instruments and calculating the scanning parameters specified by the user. The computer then sends the timing information to the RTC and moves the positioners to their initial positions. It positions the horizontal positioner at the last column and signals the RTC to start the measurements simultaneously. As the positioner moves, the RTC uses the calculated timings to precisely wait until the first element reaches the column position and then triggers the VNA. The RTC subsequently switches to the next element configuration and waits for  $\Delta t$  before triggering the VNA again. This process continues until the last element of the probe array reaches the column position. The system then moves to the next column position and repeats the process until the positioner reaches the final column. Figure 4 illustrates a general scanning grid with the measurement positions. Most linear positioners have sections in their movement that involve acceleration and deceleration. In the figure,  $A_d$  represents these sections, while  $M_d$  is the margin distance, set to  $\lambda/2$ . This margin ensures that the positioner maintains a constant speed for all elements in the first and last columns of the grid. The following equations are used to calculate the acceleration

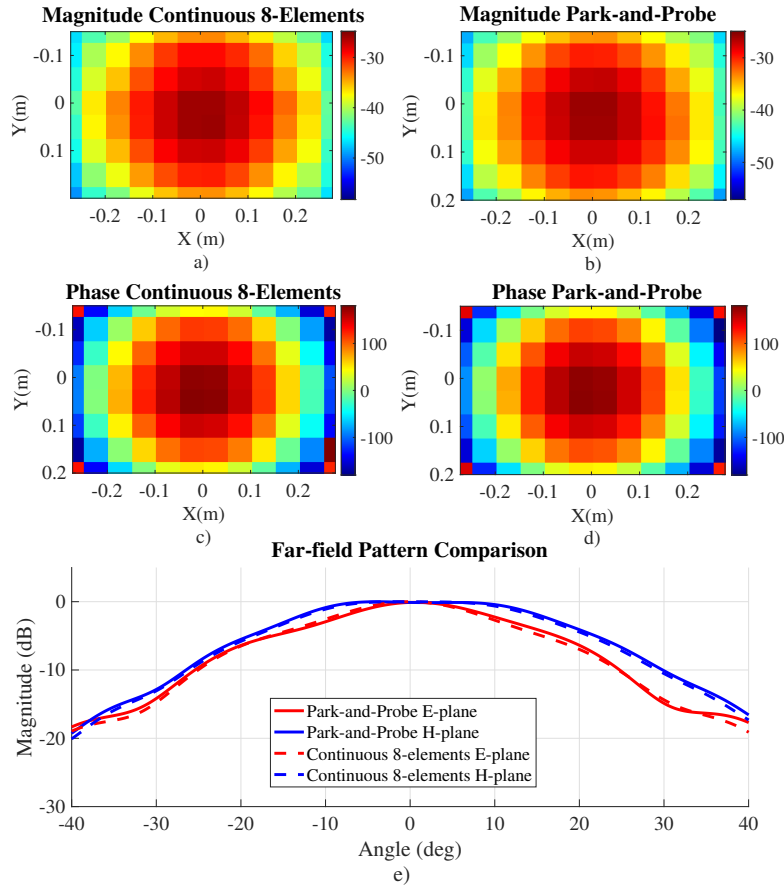


Fig. 5. Comparison of the results obtained using the park-and-probe method of scanning and the fast continuous scan with the 8-elements array probe. Displaying in a) and b) the near-field results in dB of the magnitude of the continuous 8-element test and the park-and-probe methods respectively. c) and d) is the phase results in degrees of the previous, and e) the far-field radiation pattern comparison.

distance and timing parameters.

$$A_d = \frac{v_f^2 - v_i^2}{2 \cdot a} \quad (4)$$

$$t_A = \frac{v_f - v_i}{a} \quad (5)$$

$$t_{\Delta} = \frac{d_{\Delta}}{v_f} \quad (6)$$

Where  $d_{\Delta}$  is the spacing between sampling points in the scanning grid, set to  $\lambda/2$ . The parameters  $v_f$ ,  $v_i$ , and  $a$  denote the final velocity, initial velocity, and acceleration of the linear positioner, respectively. The time  $t_A$  is the duration required for the positioner to reach the configured velocity, while  $t_{\Delta}$  is the time needed to move from one point to the next. These two values are used by the RTC to ensure accurate measurement timing.

### III. RESULTS

The primary goal of the system is to significantly reduce scanning duration while maintaining measurement reliability. Performance tests were conducted to evaluate the system's efficiency. Additionally, the system can be configured to perform different types of planar near-field scans, including

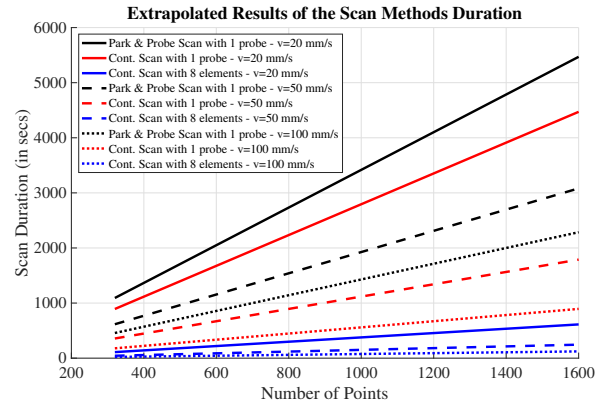


Fig. 6. Extrapolation comparison between the three methods scan duration in different positioner speed.

park-and-probe and continuous scanning with a single element. This flexibility allowed for a comparison of scan duration and performance across various configurations.

Table I compares scanning durations between the park-and-probe method, continuous scanning with a single probe, and

TABLE I  
SCAN DURATION MEASUREMENT FOR SCANS WITH A DIFFERENT  
AMOUNT OF POINTS AT 2.94 GHz AND A SPEED OF 20 mm/s

Number of Points	Scanning Range (mm)	Park-and-Probe (s)	Continuous 1 Element (s)	Continuous 8 Element (s)
96	0.55 x 0.35	318.31	292.75	34.81
192	0.55 x 0.75	638.5	587.99	85.5
288	0.55 x 1.25	NaN	NaN	136.16

continuous scanning with an 8-element probe array. For the largest scanning windows, single-probe measurements were impractical due to positioner limitations and the extensive coverage of the multi-probe array. The data show that scanning time is reduced by a factor of 9.14 for the 96-point test and by a factor of 7.46 for the 192-point test. This reduction is mainly due to the additional time required to reposition the probe array and the lower speed of the linear positioner. Measurements were taken at the maximum positioner speed of 20 mm/s. At a frequency near 3 GHz, where the half-wavelength is 50 mm, this speed is less than  $\lambda/2$ , making single-element continuous scanning only slightly faster than the park-and-probe method. Using the data from Table I, scanning durations for larger ranges were extrapolated. Although this is a simple linear approximation, it shows that the multi-probe system is significantly faster than single-probe methods. Figure 6 demonstrates that even the fastest single-probe method (100 mm/s) is slower than the slowest multi-probe scan (20 mm/s).

#### A. Scan Measurement Comparison

Using the park-and-probe method as a reference, the multi-probe system was evaluated. Figure 3 displays the system setup and the AUT, which is an S-band horn antenna used for the test. The scanning range for this test was  $0.55 \times 0.35$  m with 96 sampling points. The results are illustrated in Fig. 5. The near-field plots for both magnitude and phase are very similar, and the far-field radiation pattern measurements show only minor differences. Specifically, the E-plane has an average error of 4.68%, while the H-plane shows a 3.76% error.

#### IV. CONCLUSIONS

This design enables an irregular multi-probe system to perform continuous near-field scanning more quickly and accurately compared to other methods, reducing scanning duration by a factor of 7-9 with a percentage error of less than 5%.

There is potential for further enhancing the system's performance. Current hardware limitations restrict its effectiveness. Increasing the travel velocity with faster linear positioners could accelerate the scanning process and improve the efficiency of the switching system. The current switching time is set to 125 ms, while the array controller's minimum allowable switching time is 25 ms. Additionally, refining the array controller's design to reduce switching time and increase maximum speed, as indicated in (2), could provide further improvements.

Equations (1) and (2) are essential for designing the irregular probe array. They illustrate the relationship between frequency and the maximum speed of the linear positioner. For instance, an increase in operating frequency results in a decrease in  $\Delta d$  and requires a reduction in  $v_{max}$ . Consequently, reducing  $\Delta d$  allows the system to operate at higher frequencies but necessitates a slower linear positioner speed. This configuration might be suitable for lower frequencies but would result in longer scan durations due to the reduced maximum speed allowed by the probe array configuration.

#### ACKNOWLEDGEMENT

This work is supported by Advance Radar Research Center (ARRC), The University of Oklahoma and eMWave-tech. Any opinions, findings, conclusions, or recommendations expressed in this material are those of the author(s) and do not necessarily reflect the views of ARRC, The University of Oklahoma and eMWave-tech

#### REFERENCES

- [1] R. D. Palmer, M. B. Yearly, D. Schwartzman, J. L. Salazar-Cerreno, C. Fulton, M. McCord, B. Cheong, D. Bodine, P. Kirstetter, H. H. Sigmarsson, T.-Y. Yu, D. Zrnić, R. Kelley, J. Meier, and M. Herndon, "Horus—a fully digital polarimetric phased array radar for next-generation weather observations," *IEEE Transactions on Radar Systems*, vol. 1, pp. 96–117, 2023.
- [2] R. Palmer, D. Bodine, P. Kollias, D. Schwartzman, D. Zrnić, P.-E. Kirstetter, G. Zhang, T.-Y. Yu, M. Kumjian, B. Cheong, S. Collis, S. Frasier, C. Fulton, K. Hondl, J. Kurdzo, T. Ushio, A. Rowe, J. Salazar, S. Torres, and M. Yearly, "A primer on phased array radar technology for the atmospheric sciences," *Bulletin of the American Meteorological Society*, vol. 103, 07 2022.
- [3] F. Saccardi, A. Giacomini, L. J. Foged, N. Gross, T. Blin, P. Iversen, R. Braun, L. Shmidov, M. He, C. Chen, and X. Bland, "Experimental validation of linear multiprobe arrays for fast and accurate pnf antenna characterizations," in *2023 Antenna Measurement Techniques Association Symposium (AMTA)*, 2023, pp. 1–5.
- [4] C. Parini and S. Gregson, "Compressive sensing applied to planar near-field based array antenna diagnostics for production testing," in *2023 Antenna Measurement Techniques Association Symposium (AMTA)*, 2023, pp. 1–6.
- [5] J. A. Gordon, D. R. Novotny, M. H. Francis, R. C. Wittmann, M. L. Butler, A. E. Curtin, and J. R. Guerrieri, "Millimeter-wave near-field measurements using coordinated robotics," *IEEE Transactions on Antennas and Propagation*, vol. 63, no. 12, pp. 5351–5362, 2015.
- [6] D. R. Novotny, J. A. Gordon, M. S. Allman, J. R. Guerrieri, A. E. Curtin, K. Hassett, G. E. McAdams, and Q. Ton, "The multi-robot large antenna positioning system for over-the-air testing at the national institute of standards and technology1," 2018. [Online]. Available: <https://api.semanticscholar.org/CorpusID:173174456>
- [7] F. Saccardi, A. Giacomini, N. Gross, T. Blin, P. Iversen, R. Braun, L. Shmidov, M. He, C. Chen, X. Bland, and L. J. Foged, "Uncertainty analysis of linear multi-probe array systems for fast antenna measurements," in *2024 18th European Conference on Antennas and Propagation (EuCAP)*, 2024, pp. 1–5.
- [8] F. R. Varela, M. S. Castañer, F. Saccardi, L. Scialacqua, and L. Foged, "Planar wide mesh scanning using multi-probe systems," in *2023 Antenna Measurement Techniques Association Symposium (AMTA)*, 2023, pp. 1–5.
- [9] J. Ala-Laurinaho, S. K. Karki, V. Viikari, A. Alanne, R. Lehto, P. Moseley, and M. Simeoni, "Design of a multiprobe planar near-field scanner for ku-band," in *2023 Antenna Measurement Techniques Association Symposium (AMTA)*, 2023, pp. 1–6.
- [10] S. Gregson, J. McCormick, and C. Parini, *Principles of planar near-field antenna measurements*. IET, 2007, vol. 53.
- [11] "Waveguide sizes — dimensions cutoff frequency." [Online]. Available: <https://www.everythingrf.com/tech-resources/waveguides-sizes>